AD-A083 621   LAMONT-DOHERTY GEOLOGICAL OBSERVATORY PALISADES NY   F/G 8/10
                ACOUSTIC CHARACTERISTICS OF THE SHELVES BETWEEN ALASKA AND U.S.--ETC(U)
                OCT 79   R E HOUTZ   N00014-75-C-1126
UNCLASSIFIED   LDGO-CU-2-79   NL
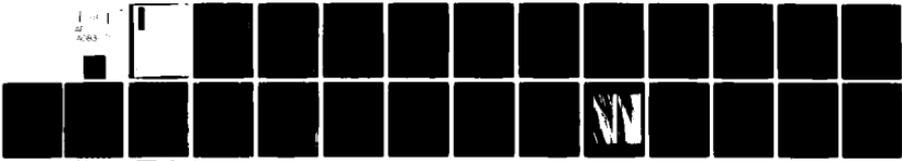
END
DATE
FILMED
5 80
DTIC

LAMONT-DOHERTY GEOLOGICAL OBSERVATORY
OF COLUMBIA UNIVERSITY
Palisades, New York 10964

T E C H N I C A L   R E P O R T

For the

EARTH PHYSICS PROGRAM

OFFICE OF NAVAL RESEARCH

Contract No. N00014-75-C-1126

ACOUSTIC CHARACTERISTICS OF THE SHELVES
BETWEEN ALASKA AND U.S.S.R.

by

Robert E. Houtz

Technical Report,

1979

DTIC
ELECTE
APR 1 7 1980
C

Introduction

Over one hundred sonobuoys were successfully deployed by the U.S. Geological Survey in the Chukchi and Beaufort seas. Owing to the thick sediments and the good quality of the sonobuoy records, the average sonobuoy yields 5 to 6 layers, ranging up to 10 layers. This work therefore provides a wealth of sound velocity information in an area where little velocity data has been published. The sonobuoys also provide good estimates of minimum sediment thickness (up to 9.6 km), some detail within the basement structure, and sea floor sound velocities.

The chart in Figure 1 shows the location of sonobuoys used in the present work. The sonobuoys obtained during 1977 and 1978 aboard R.V. Lee are indicated with open circles in Figure 1. These data were obtained with military sonobuoys (SSQ41A) and a 5-element tuned array of airguns with a total volume of 1350 in^3. Sonobuoy data were obtained during 1971, 1972, and 1973 by the U.S.C.G.C. Burton Island; these stations are shown as solid circles in the figure. They were shot with a variety of sources including mixed sources where both sparkers and airguns were used.

Generalized sediment provinces and the distribution of eroded arch s are shown in Figure 2. This map was adapted from the work of Grantz and Eittreim (1979) and Eittreim et al. (1977). The locations of the structural highs, although approximate, were used to help control contour lines of seafloor sound velocity and sediment thickness wherever control data were scarce.
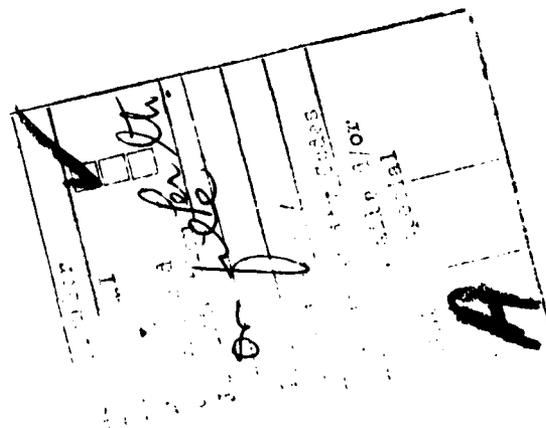
Reduction of Sonobuoy Data

The sonobuoy records shown in Figure 3 are typical of those used in the present work. For the most part the sonobuoys are located in shallow water, and the travel-time data show a smooth increase of velocity with depth, at least within the upper (sedimentary) refracted arrivals. Deep reflections are commonly observed in the shallow water sonobuoy records. Such a reflector has been labelled "R" in Figure 3. Whenever the computed reflection time to the deepest refracting layer is less than an observed reflector, the thickness of the final layer down to the reflector was computed by assuming a constant velocity equal to that of the deepest refractor. In order to compute the thickness as accurately as possible, in sediments whose velocity increases smoothly with depth, it is necessary to pick as many velocity changes as possible. As a consequence, many of our solutions contain upwards of 10 layers. As a check against these thickness calculations, twelve sonobuoys with well-defined travel-time curvature (without velocity cusps) were inverted by use of the Herglotz-Bateman velocity inversion technique. One such sonobuoy is shown in the left hand side of Figure 3. These results will be discussed in more detail later, but it can be mentioned here that the depths computed from closely spaced refraction picks are in good agreement with the inverted data.

After studying the sonobuoy records it was concluded that the onsets of the low-energy, straight-line refraction arrivals generally occurred at velocities equal to or greater than about 4.5 km/s. At shallower depths the travel-time data are curved, and since they benefit from the focussing effect of a positive velocity gradient, they contain

much more energy. These properties are rather easily identified (see the arrow on the left of Fig. 3) and are the basis for division into 'basement' and sediment in our sections, although the work of Grantz et al., show that over most of the shelf, basement defined in this way is actually sedimentary.

It seems to be a characteristic of shelf sediments whose velocities increase smoothly with depth that dipping reflectors (bedding planes) have little or no effect on the refraction velocity. That is to say, zones of equal sound velocity tend to be horizontal in spite of dipping bedding planes (cf. Houtz and Davey, 1973). This is shown in Figure 4 where sonobuoys 32 and 34 are only a few miles apart: 32 was shot up-dip and 34 was shot down-dip, yet there are no important differences between their velocity structures. Dip corrections have been applied to basement velocities, but only in the very few areas where large velocity contrasts exist between sediment and basement. Typically the contrast is less than 400 m/s and the correction is hardly more than the accuracy of measurement. The independence of refraction velocities from bedding plane dip is a convenient demonstration that simple overburden controls velocity. This implies a lack of significant pelagic content, such as lime or silica, which would yield cemented layers whose refraction velocity would be affected by the dip.

Standard T^2/X^2 techniques were applied to the deep water sonobuoy data in the Canada basin. These solutions, based on variable-angle reflections, yield interval velocities. These solutions are dependent on the dip of the reflectors and must be carefully corrected. All the sonobuoy solutions from the present work are listed in Table 1. Except for a

few deep-water stations, all the sonobuoy solutions are based on conventional refraction techniques.

Sound Velocity Analysis of Sediments

Velocity-depth information was collected from eight regions in the study area where the sediments are thick enough to make meaningful statistical correlations between velocity and depth. The solutions for layer thickness from these areas were converted to time, and each velocity was assigned to the mid-point (in units of one-way travel time) of its layer. Least-squares lines were fitted to the velocity-time data to yield the regression coefficients, standard error of estimate, and correlation coefficient. Results are shown in Figure 5 where each region is outlined and labelled, and the statistical information is listed. Whenever possible, refraction velocities greater than 4.5 km/s were included in the velocity-depth plots, but most of these points fell well above the regression line and cannot be included. Their rejection on the basis of their reduced amplitudes and relative lack of travel-time curvature, as discussed earlier, seems to have been justified.

The velocity data from the western Beaufort sea (areas B, C, D) are similar enough to indicate a common origin, whereas the Canada basin to the north (area E) has a much lower velocity gradient in deep water sediments. The distributions from these study areas have large correlation coefficients, indicating thick and uniform sediments. Areas A and G are identical, but quite distinct from BCD. The principal difference between the two groups is the 40% increase in the acceleration factor (K) in area AG over that of BCD. This difference may only represent

the contrast between proximal (western Beaufort shelf) and distal (North Chukchi basin) sedimentation of materials that are otherwise about the same age and with the same type of provenance.

Earlier results obtained by Hofer and Varga (1972) from Mackenzie Bay 100 km east of area D, show a gradual increase of velocity with depth. Their measurements were based on carefully correlated stacking velocities. The velocity–depth distribution indicated to them that the sediments were likely to be a 'sand-shale sequence of Tertiary and Cretaceous age', whose properties they correlated with on-shore well-log data. They obtained the relation $v = 1.62 + 1.39 t$ in a single survey line, which compares very favorably with our results: $v = 1.59 + 1.53 t$ from area D.

During the reduction of the sonobuoy data, it was apparent that many of the records could be more accurately reduced by considering the travel-times as continuously varying rather than as straight line segments. In order to use velocity inversion techniques with a minimum of error, we chose travel-time plots that are devoid of prominent velocity cusps (small cusps, i.e. short 'reversed segments' are not easily identified and have no important effect on the inversions). An example of a prominent velocity cusp appears in the right side of Figure 3, which shows that the high-energy cusp survives the multiple reflection process, whereas the deeper straight-line refraction segment is too weak to persist beyond the first multiple. The water layer multiples of the retrograde and prograde portions of the cusp are labelled A and B, respectively, in the figure. After selecting only those records with

relatively deep ray excursions (maximum depths range from 2.5 to 4 km), and screening those with velocity cusps, 12 high-quality records were inverted by means of the Herglotz-Bateman technique.

These inversions were originally carried out as a check against the conventional refraction solutions, which could yield inaccurate results in a sediment column whose velocity increases smoothly with depth. It was found, however, that there are only random differences between the two techniques if 'layers', as picked from the records, are separated by velocity differences of about 300 m/s. It is worth noting that picking layers that are thin relative to a wavelength in a velocity-depth continuum is entirely valid. Objections are raised if conventional refraction methods are used on thin layers, but no objections are raised if the same procedure is called a tau-p inversion, even though the results and the computing procedures are the same.

The velocity inversions seem to provide additional information if they are plotted in their geographical setting, as portrayed in Figure 5 with insets and lines connecting the plots to the sonobuoy station location. It can be seen that area B velocity-depth plots are all basically linear, whereas those from some of the other areas are more complex, and consist of velocity-depth curves or two quite different linear segments. In each case the near-surface linear segment has a greater velocity gradient than in the deeper one. The change-over point from a high to a low velocity gradient occurs fairly consistently at a velocity of about 3 km/s, but the depth at which this occurs is quite variable.

The interval velocity solutions of Hofer and Varga show a very pro-

nounced change in velocity gradient at 3.0 km/s. This event is associated in their data with a moderately strong reflector within a uniform sedimentary sequence. A spot check of our own records revealed no consistent relation between the vertical reflection records and the change of gradient. Although this change of gradient is important to geo-acoustic modelling, our data do not show it as an identifiable geologic event.

The linearity of the velocity-depth plots from area B indicates that the data would be better fitted with a least-squares line relating velocity and depth (rather than one-way travel-time). However, the standard error of estimate and the correlation coefficient actually degrade when a linear relation is attempted between velocity and depth. These results show that the sonobuoys with linear increases of velocity with depth are not representative of the general velocity structure within area B. (The use of a velocity-time regression, although it produces a curved depth distribution, does not increase the degrees of freedom because both the time and depth regressions are compared in their linear forms.)

Seafloor sound velocities in the study area are contoured in Figure 6. These values were determined by picking the earliest possible head-waves in the sonobuoy records. The first layer picks for the thickness calculations were picked from longer refracting segments and are therefore better representative of the 'layer' velocity, but such velocities are somewhat higher than the estimated seafloor sound velocity. As it turns out the velocity-depth functions projected to the seafloor tend to

yield velocities that are in good agreement with the uppermost headwave values plotted in Figure 6. These statistical projections to the sea-floor can sometimes be unrealistic.

A third method has been developed to estimate seafloor sound velocity from multiple seafloor reflections at critical incidence. These reflections and their multiples form the line labelled V_g in the right hand side of Figure 3. The group velocity, V_g, can be converted to seafloor sound velocity with a very simple calculation (Sutton and Maynard, 1971). This method yields an average seafloor velocity of 1.63 km/s (based on 8 observations) in areas B, C, and D; and 1.73 km/s (3 observations) from area G. These values are in convincing agreement with the average values based on uppermost headwaves (cf. Fig. 6).

The distribution of seafloor sound velocities shows an increase in velocity in the region of structural arches. This is quite apparent in the central Chukchi sea where the arch is actually an overthrust (Grantz and Eittreim). The minimum velocities are observed on the outward-building, seaward edges of the shelves, and in the central part of the interior basin. An elongate belt of relatively fast velocities are contoured just west of Mackenzie Bay, which may correspond to the 'broad mid-shelf arches and anticlines expressed in Neogene beds' reported here by Grantz and Eittreim.

Area H (Fig. 5) is quite distinct from the other thick sedimentary accumulations because the seafloor sound velocities here are unusually high. This can be seen in Figure 6, but also in the intercept value of

the Area H velocity function. This seems to be directly related to the
fact that area H (foredeep) sediments are no younger than Lower Cretaceous,
whereas all the other thick sediments are capped by Neogene sediments
that are usually quite thick.

Sediment Distribution

The sediment isopach map in Figure 7 is contoured in units of depth
down through velocities of 4.5 km/s. Materials faster than this are
sedimentary, but they have rather low velocity gradients, so that they
are conveniently separable. The isopach map has been contoured to
conform with the generalized structure shown in Figure 2. The sonobuoy
solutions have been supplemented with results from Eittreim et al.,
(1977), Grantz and Eittreim (1979), and Eittreim and Grantz (in press).
The additional data were obtained from CDP results and some of their
earlier interpretations of the sonobuoys listed in Table 1. These
earlier solutions are in good agreement with the results listed in Table
1. They were used to identify reflecting surfaces with refraction
velocities greater than 4.5 km/s, which I then extrapolated to add to
the number of points to be contoured.

The contours on the southernmost arch are based on the sections of
Eittreim et al., which they computed with a velocity function of v =
1.72 + 2.02 t. However, Eittreim (in preparation) has now revised his
estimate downwards, based on an extensive sampling of CDP solutions.
His latest velocity function is shown in Figure 5, and is preferable
to the very small sample available in the present work.

The contoured depths to layers with refraction velocity greater than 4.5 km/s do not necessarily represent a geological boundary. This is especially true on the western Beaufort shelf near Mackenzie Bay, where the 4.5 km/s refraction velocity is observed at depths of about 3 km sub-bottom, which cuts across Lower Tertiary to Jurassic fold structures.

Constraints on the Near-Seafloor Data

A comparison of the velocity depth plots in Figure 5 shows that the near-seafloor velocity gradients will be largest where the velocity plots are non-linear. Where the plots are linear, the regional velocity functions are fairly reliable. However, there is good evidence in area H and to some extent elsewhere on the northern Chukchi shelf, that the near surface velocity gradients may be somewhat more than that predicted by the velocity functions. Ideally the travel-time data from each sonobuoy would be inverted, but the labor of doing so, at present is beyond the scope of this paper.

The present work has demonstrated again that random geophysical measurements, such as seafloor sound velocity become more coherent when considered within the constraints of the regional geology. An example that comes to mind here is the elongate gentle fold on the western Beaufort shelf whose crests show up as a 200 m/s increase in the seafloor sound velocity. Similarly Area H, the Colville foredeep, has seafloor sound velocities that are 300 to 400 m/s faster than those in the other basins; this is directly related to their Cretaceous age compared to the much younger sediments in the other basins.

REFERENCES

Eittreim, S., A. Grantz, and O. Whitney, Cenozoic sedimentation and tectonics of Hope basin, southern Chukchi sea, in The Relationship of Plate Tectonics to Alaskan Geology and Resources, edited by A. Sisson, Alaska Geol. Soc., Anchorage, 1977.

Eittreim, S., and A. Grantz, in Crustal Properties across Passive continental Margins, edited by C. Keen and M. Keen, Special Vol. Tectonophysics (in press).

Grantz, A., and S. Eittreim, Geology and physiography of the continental margin north of Alaska and implications for the origin of the Canada basin, U.S. Geol. Survey Open-File Report 79-288, 1979.

Hofer, H., and W. Varga, Sesimogeologic experience in the Beaufort sea, Geophysics, v. 37, no. 4, p. 605-619, 1972.

Houtz, R., and F. Davey, Seismic profiler and sonobuoy measurements in Ross Sea, Antarctica, J. Geophys. Res., 78, 3448-3468, 1973.

Sutton, G., and L. Maynard, Ocean-Bottom sediment velocity determined from critical range multiple reflections (abstract only), EOS, 52, 4, 1971.

Station	H1	H2	H3	H4	H5	H6	H7	H8	H9
2B71	.02	.20	.34	.21	.41	.22			
4	.05	.60	.69	2.63					
5	.05	.48	.37	.26	.39	.46			
6	.05	.20							
8	.05	.53	.39	.34					
9	.05	.35	.38	.54	.59	.57			
13	.04	.25	.23						
14	.05	.34							
1B72	.07	.51							
2	.05	.14	.23	.41					
4	.08	.28	.48	.51	.50				
5	.09	.58	.31	.62	.18	.81			
6	.04	.23	.13	.38	.24	.43			
7	.04	.15	.25	.38	.37				
8	.05	.08	.52	.45	.38	.37	.45		
2B73	.04	.47	.18	.43	.32	.38	.73		
3	.03	.32							
5	.15	.41	.28	.34					
2L6	.05	.48	.47						
3	.03	.28	1.56						
4	.04	.26	.41	.48	1.33	3.35	1.60		
5	.04	.45	.38	1.24	3.51				
6	.06	.29	.41	4.06					
7	.21	.25	.49	.64	.83	1.77	2.58		
8	.03	.60	.89						
9	.03	1.01	1.02						
10	.04	1.92	.04						
11	.02	.25	.80	.87	3.08				
13	.02	.38	.55	.57	.76				
16	.02	.59	.44	.78	.67				
17	.04	.63	.66	.82	.76	.92			
21	.02	.25	.78	.95	.87	2.05			
22	.03	.85	.62	1.14	3.30				
23	.03	.56	.65	.59					
24	.03								
25	.03	1.16	.72	1.72	2.44				
27	.03	.53	.66	.89	1.38	(4.85)			
28	.06	.75	.49	.77	.59	1.02	1.21		
29	.02	.20	.44	.45	.85	3.91			
30	.02	.36	.31	.51	.79	1.42	2.33		
31	.02	.75	.57	.85	.97	1.20	1.34	3.23	(2.14)
32	.02	.74	.41	.57	.87	1.10	.75	1.41	
33	.02	.36	.58	.66	.48	2.10			
34	.02	.84	.42						
35	.02	1.74	2.32						
36	.05								
37	.05	.61							
39	.03	.69	.69	.65	1.25	1.52	3.34		
2L9	.03	.58	.53	.43	.47	.57			
5	3.39	1.23	.48	.43	.50	1.22			
6	3.23	.58	.35	.37	.71	.56	1.50		
7	2.72	.92	.70						
9	2.66	.64	1.02	.81	2.40				
11	2.46	.74	.85	.74					
13	.03	.70	.52	.56	.48	.76	.87	4.23	
14	2.83	.78	.60	1.58	2.61	4.00			
19	.04	.66	.60	.65	1.03				
22	3.27	1.12	1.89						
25	.03	.82	.30	.36	.59	.91			
27	.04	.13	.26	.53	.58				
30	.05	.63	.30	.35	.34	1.02	2.38		
31	.05	.54	.34	.26	.39	.49	2.64		

7	.04	.15	.25	.38	.37				
8	.05	.08	.52	.45	.38	.37	.45		
2B73	.04	.47	.18	.43	.32	.38	.73		
3	.03	.32							
5	.15	.41	.28	.34					
2L6	.05	.48	.47						
3	.03	.28	1.56						
4	.04	.26	.41	.48	1.33	3.35	1.60		
5	.04	.45	.38	1.24	3.51				
6	.06	.29	.41	4.06					
7	.21	.25	.49	.64	.83	1.77	2.58		
8	.03	.60	.89						
9	.03	1.01	1.02						
10	.04	1.92	.04						
11	.02	.25	.80	.87	3.08				
13	.02	.38	.55	.57	.76				
16	.02	.59	.44	.78	.67				
17	.04	.63	.66	.82	.76	.92			
21	.02	.25	.78	.95	.87	2.05			
22	.03	.85	.62	1.14	3.30				
23	.03	.56	.65	.59					
24	.03								
25	.03	1.16	.72	1.72	2.44				
27	.03	.53	.66	.89	1.38	(4.85)			
28	.06	.75	.49	.77	.59	1.02	1.21		
29	.02	.20	.44	.45	.85	3.91			
30	.02	.36	.31	.51	.79	1.42	2.33		
31	.02	.75	.57	.85	.97	1.20	1.34	3.23	(2.14)
32	.02	.74	.41	.57	.87	1.10		.75	1.41
33	.02	.36	.58	.66	.48	2.10			
34	.02	.84	.42						
35	.02	1.74	2.32						
36	.05								
37	.05	.61							
39	.03	.69	.69	.65	1.25	1.52	3.34		
2L9	.03	.58	.53	.43	.47	.57			
5	3.39	1.23	.48	.43	.50	1.22			
6	3.23	.58	.35	.37	.71	.56	1.50		
7	2.72	.92	.70						
9	2.66	.64	1.02	.81	2.40				
11	2.46	.74	.85	.74					
13	.03	.70	.52	.56	.48	.76	.87	4.23	
1?	2.83	.78	.60	1.58	2.61	4.00			
19	.04	.66	.60	.65	1.03				
22	3.27	1.12	1.89						
25	.03	.82	.30	.36	.59	.91			
27	.04	.13	.26	.53	.58				
30	.05	.63	.30	.35	.34	1.02	2.38		
31	.05	.54	.34	.26	.39	.49	2.64		
32	.06	.66	.45	.47	.62	.75	.73	1.11	
33	.03	.81	.50	.51	.77	1.39	2.40		
34	.05	.67	.54	.33	.46	.72			
36	.05	.78	.26	.53	.72	.59	3.89		
38	.04	.76	.40	.80	2.15.	2.07	5.50		
39	.03	.79	.53	1.22	1.21	2.92			
40	.03	.60	.80	.80	.85				
41	.04	.77	.52	.59	.79	.77	1.54	5.25	
43	.05	.82	.51	.72	.66	.62	1.18		
44	.04	1.11	.57	1.07					
45	.05	.29	.40	.76	.80				
46	3.07	.73	1.00	1.19					

2.

CHUKCHI SEAS

V2	V3	km/s V4	V5	V6	V7	V8	V9	North Lat.	West Long.
2.20	2.70	3.00	3.25	3.40	3.65			70-43	161-05
1.85	2.50	5.70	7.20					71-23	167-40
2.10	2.70	3.00	3.45	3.85	4.20			70-35	167-15
2.95	3.70							69-55	167-35
1.85	2.30	2.65	4.65					68-36	168-17
1.75	2.05	2.40	2.80	3.10	4.20			67-45	167-51
1.85	2.70	3.15						70-56	169-30
1.70	2.40							70-56	167-17
1.80	2.20							72-29	159-00
2.00	2.70	3.20	4.20					71-33	159-00
1.75	2.00	2.45	2.80	3.00				72-55	161-00
1.85	2.20	2.60	2.80	3.00	3.70			73-06	163-10
2.00	2.40	2.70	3.05	3.45	3.75			71-05	163-00
1.75	2.00	2.20	2.40	2.65				73-08	166-30
1.75	2.00	2.35	2.65	3.00	3.35	3.80		72-42	168-00
1.90	2.05	2.30	2.55	2.80	3.10	3.95		71-04	150-55
1.75	1.90							71-05	153-00
1.75	1.95	2.30	2.55					71-40	154-05
1.85	2.10	4.40						68-54	168-04
2.95	3.60	4.05						69-24	165-49
2.20	2.80	3.15	3.80	4.25	5.30	5.80		70-34	162-27
2.30	3.15	4.75	5.15	5.70				71-36	159-23
2.20	2.85	4.50	6.25					71-41	159-30
1.80	2.45	2.90	3.60	4.10	4.70	5.60		70-42	165-04
(1.9)	5.20	5.80						69-24	168-21
3.90	4.75	5.30						69-40	169-24
3.60	4.15	6.30						70-20	168-59
2.15	3.00	3.65	5.65	6.55				70-43	168-12
1.80	2.25	3.00	3.40	5.60				71-05	167-26
1.85	2.50	3.05	3.60	5.10				71-29	166-34
1.90	2.40	3.05	3.50	4.10	5.25			71-48	165-47
1.80	2.15	3.05	3.60	4.60	5.60			72-39	164-38
2.10	2.45	3.50	4.35	5.15				72-24	166-31
2.00	2.45	3.05	5.95					71-38	169-25
3.75								70-34	171-39
2.15	3.10	3.90	4.70	5.60				72-13	171-23
1.85	2.35	3.15	3.85	4.45				72-26	173-31
1.95	2.55	3.05	3.50	4.00	4.50	4.85		72-55	175-50
2.10	2.70	3.20	3.60	4.20	5.05			70-37	162-03
2.05	2.60	3.00	3.50	3.90	4.40	5.00		70-46	163-31
1.90	2.65	3.30	3.65	4.20	4.80	5.45	6.10	70-56	165-01
1.85	2.55	3.00	3.60	4.15	4.60	5.00	6.60	71-00	166-02
1.75	2.25	2.90	3.40	5.50	6.45			71-06	167-13
2.35	2.85	6.15						71-11	168-33
4.85	5.40	5.90						70-04	170-45
4.80								70-00	170-45
4.30	4.75							69-44	170-50
1.80	2.25	3.00	3.75	5.35	6.00	7.20		68-13	170-45
1.65	2.05	2.40	2.80	3.70	4.45			67-21	166-35
2.05	2.36	2.59	2.61	3.58				72-33	144-49
1.88	2.14	2.25	2.74	2.63	3.25	4.20		72-21	143-27
2.15	2.27							71-50	141-00
2.00	2.35	2.89	3.48					71-43	141-00
2.07	2.08	2.39	3.35					71-18	140-58
1.80	2.25	3.00	3.40	5.60				69-50	141-18
1.89	2.27	(3.0)	3.65	4.40	5.30			71-34	142-04
2.00	2.20	2.80	3.30	4.10				70-14	142-50
2.18	2.90	3.50						71-45	144-43
2.00	2.30	2.80	3.25	3.70	4.30			70-15	144-25
1.60	2.20	2.60	3.60	4.30				70-16	143-31
1.75	2.00	2.25	2.60	2.90	3.35	4.30		70-28	140-59
1.90	2.10	2.40	2.65	2.95	3.35	3.85		70-09	141-33

```
1.75  2.00    2.20 2.40 2.65                    73-08  166-30
1.75  2.00    2.35 2.65 3.00 3.35 3.80          72-42  168-00
1.90  2.05    2.30 2.55 2.80 3.10 3.95          71-04  150-55
1.75  1.90                                       71-05  153-00
1.75  1.95    2.30 2.55                          71-40  154-05
1.85  2.10    4.40                               68-54  168-04
2.95  3.60    4.05                               69-24  165-49
2.20  2.80    3.15 3.80 4.25 5.30 5.80          70-34  162-27
2.30  3.15    4.75 5.15 5.70                     71-36  159-23
2.20  2.85    4.50 6.25                          71-41  159-30
1.80  2.45    2.90 3.60 4.10 4.70 5.60          70-42  165-04
(1.9) 5.20    5.80                               69-24  168-21
3.90  4.75    5.30                               69-40  169-24
3.60  4.15    6.30                               70-20  168-59
2.15  3.00    3.65 5.65 6.55                     70-43  168-12
1.80  2.25    3.00 3.40 5.60                     71-05  167-26
1.85  2.50    3.05 3.60 5.10                     71-29  166-34
1.90  2.40    3.05 3.50 4.10 5.25               71-48  165-47
1.80  2.15    3.05 3.60 4.60 5.60               72-39  164-38
2.10  2.45    3.50 4.35 5.15                     72-24  166-31
2.00  2.45    3.05 5.95                          71-38  169-25
3.75                                             70-34  171-39
2.15  3.10    3.90 4.70 5.60                     72-13  171-23
1.85  2.35    3.15 3.85 4.45                     72-26  173-31
1.95  2.55    3.05 3.50 4.00 4.50 4.85          72-55  175-50
2.10  2.70    3.20 3.60 4.20 5.05               70-37  162-03
2.05  2.60    3.00 3.50 3.90 4.40 5.00          70-46  163-31
1.90  2.65    3.30 3.65 4.20 4.80 5.45 6.10     70-56  165-01
1.85  2.55    3.00 3.60 4.15 4.60 5.00 6.60     71-00  166-02
1.75  2.25    2.90 3.40 5.50 6.45               71-06  167-13
2.35  2.85    6.15                               71-11  168-33
4.85  5.40    5.90                               70-04  170-45
4.80                                             70-00  170-45
4.30  4.75                                       69-44  170-50
1.80  2.25    3.00 3.75 5.35 6.00 7.20          68-13  170-45
1.65  2.05    2.40 2.80 3.70 4.45               67-21  166-35
2.05  2.36    2.59 2.61 3.58                     72-33  144-49
1.88  2.14    2.25 2.74 2.63 3.25 4.20          72-21  143-27
2.15  2.27                                       71-50  141-00
2.00  2.35    2.89 3.48                          71-43  141-00
2.07  2.08    2.39 3.35                          71-18  140-58
1.80  2.25    3.00 3.40 5.60                     69-50  141-18
1.89  2.27    (3.0)3.65 4.40 5.30               71-34  142-04
2.00  2.20    2.80 3.30 4.10                     70-14  142-50
2.18  2.90    3.50                               71-45  144-43
2.00  2.30    2.80 3.25 3.70 4.30               70-15  144-25
1.60  2.20    2.60 3.60 4.30                     70-16  143-31
1.75  2.00    2.25 2.60 2.90 3.35 4.30          70-28  140-59
1.80  2.10    2.40 2.65 2.95 3.35 3.85          70-09  141-33
1.85  2.05    2.25 2.65 3.00 3.35 3.85 4.30     70-22  142-16
1.90  2.15    2.55 2.90 3.20 4.20 5.00          69-58  142-01
1.80  2.00    2.35 2.60 3.00 3.35               70-15  142-01
2.00  2.30    2.70 3.05 3.45 4.35 5.60          70-24  143-17
1.85  2.15    2.70 3.55 4.10 4.80 5.30          70-24  145-13
1.95  2.50    3.20 4.00 4.35 4.70               70-13  145-29
1.70  2.00    2.65 3.10 3.75                     70-46  146-25
1.85  2.10    2.40 2.95 3.50 4.30 4.75 5.50     70-37  146-38
1.80  2.25    2.55 3.10 3.60 4.15 4.65          70-48  146-55
1.80  2.10    3.10 3.80                          70-46  147-33
(1.8) 2.05    2.35 2.90 3.40                     70-53  147-23
1.91  2.64    3.38 3.75                          71-35  146-25
```

Station	H1	H2	H3	H4	H5	H6	H7	H8	H9	V2	V3	V4	V5
47	.05	.39	.40	.62	.47	.72				1.80	2.05	2.25	3.
48	.04	.60	.62	.65	.21					1.90	2.15	2.80	3.
49	.05	1.01	.99	(3.75)						1.90	2.70	3.70	
50	.07	.86	.95	1.16	2.17	3.60				1.95	2.35	3.55	4.
51	.05	.35	.36	.41	.51	.50	.75	2.07		1.75	2.00	2.30	2.
53	.04	.44	.55	.56	.56	(2.70)				1.90	2.20	2.40	2.
54	.03	.80	.61	.64	.55	.61	1.04	3.74		1.95	2.15	3.10	3.
57	.04	.53	.83	.64	.71	4.05	2.98			1.80	2.20	2.90	3.
58	.04	.51	.92	.91	1.73	5.47				1.95	2.15	3.00	3.
60	.05	.54	1.24	.70	.89	(4.51)				1.85	2.25	3.15	3.
62	.06	.46	.50	.62	.64	.58				1.75	2.10	2.60	3.
63	.03	.46	.44	.70	1.20	2.64				1.70	2.10	2.50	3.
64	1.95	1.09	.99	.74						(1.8)	2.35	3.30	3.
65	.06	.29	.35	.73	.29	.38	.52			1.75	2.05	2.30	2.
66	.06	.46	.32	.42	.41	.51	.40			1.70	1.95	2.30	2.
67	.04	.32	.38	.31	.34	.43	.38			1.80	2.10	2.30	2.
68	.04	.33	.36	.37	.47	.54	.67			1.65	1.95	2.20	2.
69	.05	.66	.40	.76	.96	2.70	(3.07)			2.00	2.25	2.60	3.
70	.09	.35	.24	.27	.30	.39	.54	.60		1.70	2.00	2.40	2.
71	.03	.58	.27	.47	.54	.52	1.07	.26		1.75	2.00	2.45	3.
72	.04	.49	.65	.58	1.06					1.75	2.05	2.75	3.
73	.08	.60	.37	.33	.35	.76				1.80	2.15	2.40	2.
74	.09	.47	.38	.35	.59	.45	.73	1.48	1.14	1.70	1.95	2.20	2.
75	.06	.43	.52	.52	.64	.65	1.06	(5.22)		1.70	2.00	2.45	2.
77	.05	.49	.47	.35	1.10	1.05	4.76	2.61		1.85	2.10	2.45	2.
78	.05	.72	.44	.50	.75	.83	1.45			1.90	2.30	2.70	3.
79	.18	.58	.43	1.15						1.80	2.40	2.75	3.
80	.06	.41	.45	.92	2.18	1.26				1.80	2.45	3.20	4.
83	.06	.47	.47	2.77	(3.56)					2.20	2.80	4.15	5.
85	.12	.30	.74							2.35	2.75	5.10	

| H6	H7	H8	H9	V2	V3	V4	V5	V6	V7	V8	V9	North Lat.	West Long.
.72				1.80	2.05	2.25	3.05	3.30	3.60			70-57	148-20
				1.90	2.15	2.80	3.10	3.50				70-57	149-01
				1.90	2.70	3.70						71-10	149-17
.60				1.95	2.35	3.55	4.30	5.00	6.20			71-12	150-18
.50	.75	2.07		1.75	2.00	2.30	2.75	3.00	3.35	3.95	6.15	71-08	150-25
(2.70)				1.90	2.20	2.40	2.70	3.35				71-00	149-11
.61	1.04	3.74		1.95	2.15	3.10	3.40	3.80	4.40	4.80	5.40	70-56	148-43
.05	2.98			1.80	2.20	2.90	3.45	3.95	4.70	5.15		70-47	147-41
.47				1.95	2.15	3.00	3.90	4.50	5.15			70-42	147-00
(4.51)				1.85	2.25	3.15	3.85	4.40				70-31	145-32
.58				1.75	2.10	2.60	3.10	3.50	4.00			71-17	151-14
.64				1.70	2.10	2.50	3.30	4.25	5.50			71-09	151-52
				(1.8)	2.35	3.30	3.90					71-56	151-52
.38	.52			1.75	2.05	2.30	2.50	2.75	3.15	3.55		71-34	153-03
.51	.40			1.70	1.95	2.30	2.65	3.15	3.50	3.75		71-27	153-11
.43	.38			1.80	2.10	2.30	2.65	3.05	3.50	3.85		71-16	153-39
.54	.67			1.65	1.95	2.20	2.50	3.00	3.50	4.00		71-26	154-08
2.70	(3.07)			2.00	2.25	2.60	3.30	3.80	4.30			71-39	154-22
.39	.54	.60		1.70	2.00	2.40	2.75	3.10	3.50	3.85	4.60	71-34	155-32
.52	1.07	.26		1.75	2.00	2.45	3.00	3.45	3.80	4.25	4.80	71-32	154-59
				1.75	2.05	2.75	3.35	3.75				71-38	154-16
.76				1.80	2.15	2.40	2.80	3.20	3.55			71-25	153-38
.45	.73	1.48	1.14	1,70	1.95	2.20	2.65	3.05	3.50	4.10	4.45/5.10	71-22	153-01
.65	1.06	(5.22)		1.70	2.00	2.45	2.90	3.50	4.00	4.35		71-19	152-19
1.05	4.76	2.61		1.85	2.10	2.45	2.85	3.80	4.40	5.45	6.35	71-15	151-36
.83	1.45			1.90	2.30	2.70	3.10	3.75	4.15	4.45		71-12	150-58
				1.80	2.40	2.75	3.85					72-34	158-04
1.26				1.80	2.45	3.20	4.50	6.00	7.30			72-25	158-29
)				2.20	2.80	4.15	5.35					71-40	158-20
				2.35	2.75	5.10						71-26	157-30
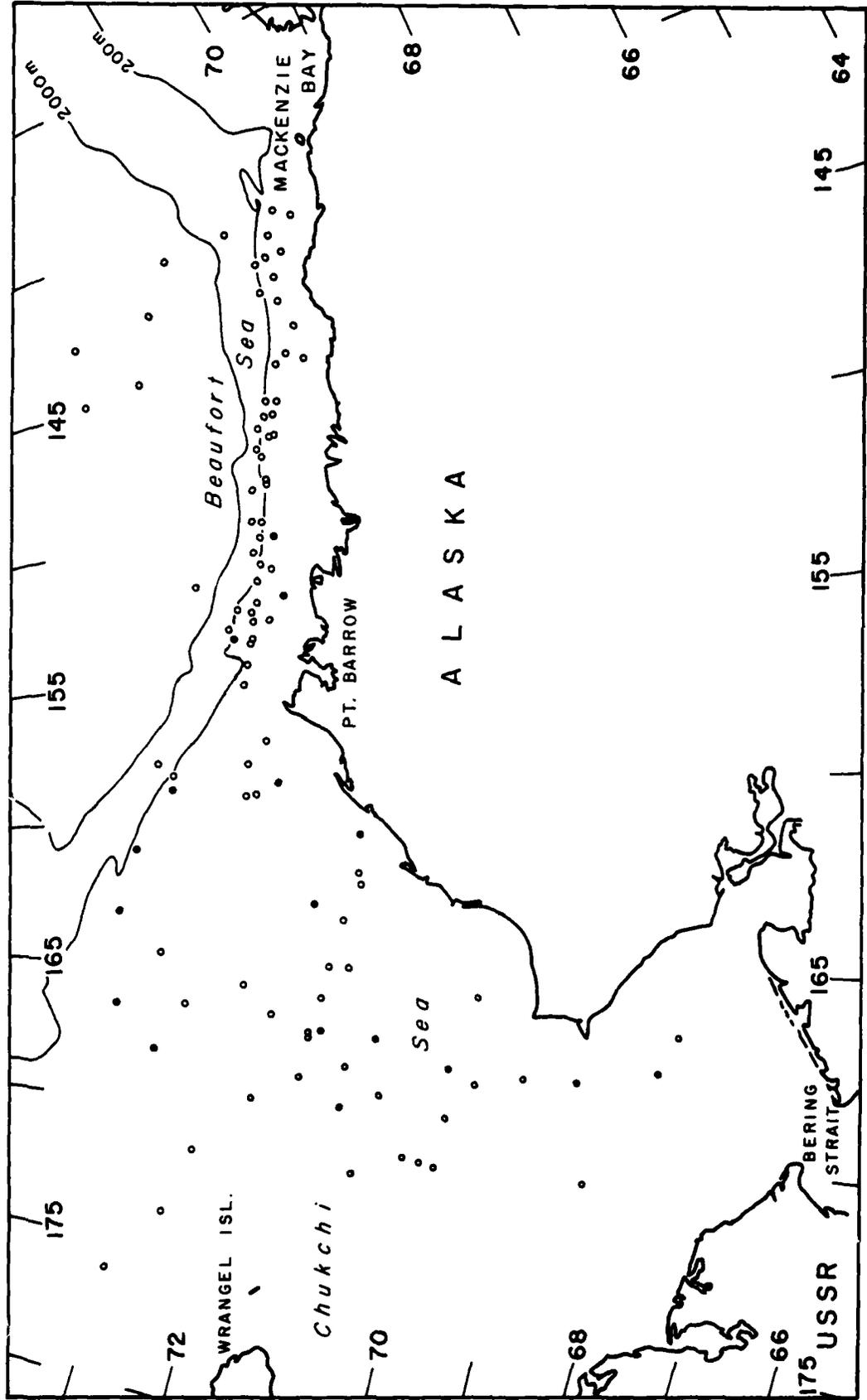
Fig. 1. Locations of sonobuoys and geographical names in study area.
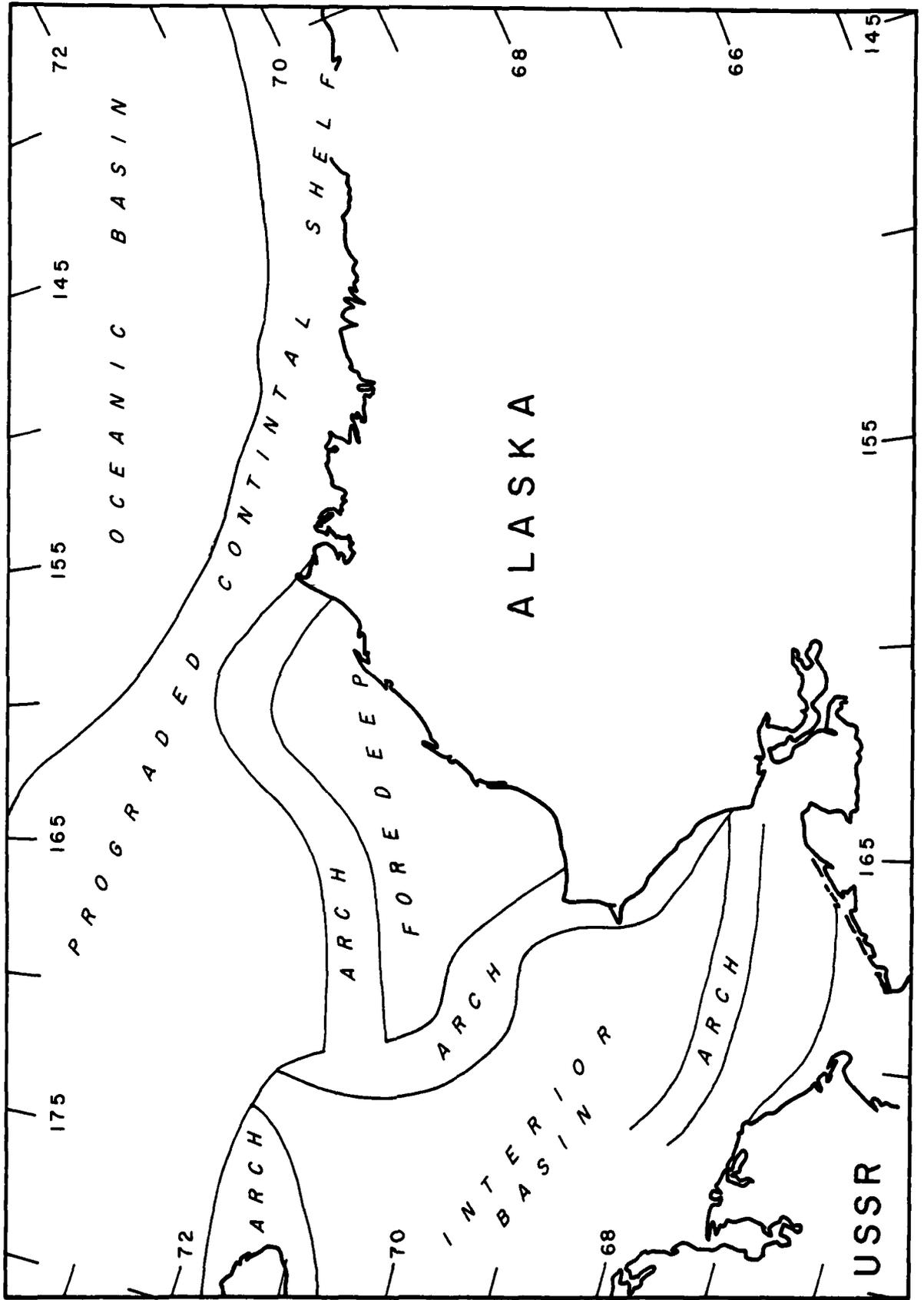
Fig. 2. Geological provinces between Alaska and U.S.S.R.

26 KM **28.5 KM**
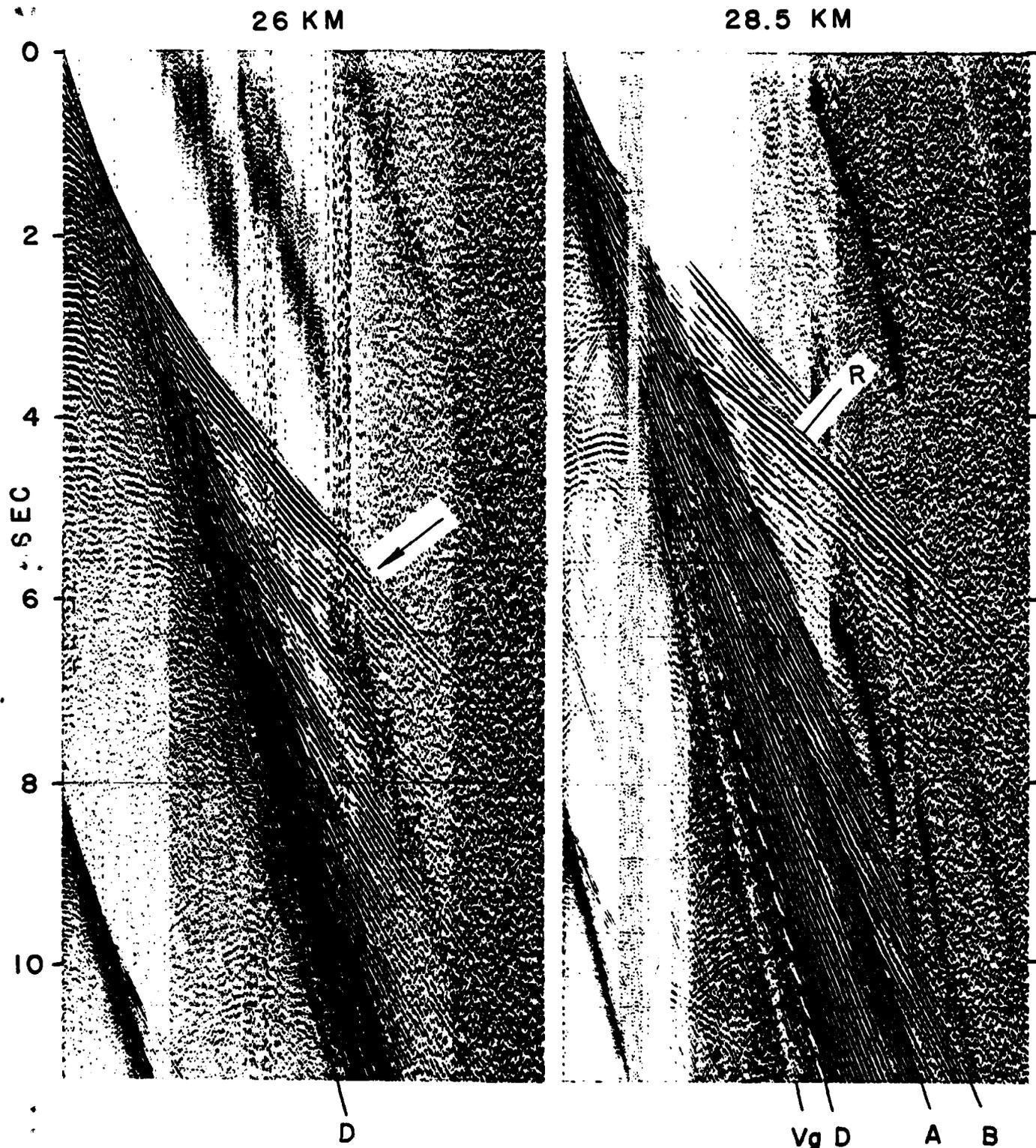
Fig. 3. Sonobuoy records from Chukchi sea. Record on left shows the transition, marked by an arrow, between curved upper portion of travel-time plot and the weaker straight-line refraction. Deep reflector labelled 'R' on the right. Water layer multiples of critical seafloor reflections (V_g) and prograde and retrograde branches of velocity cusp (B and A, respectively) are identified on the right.
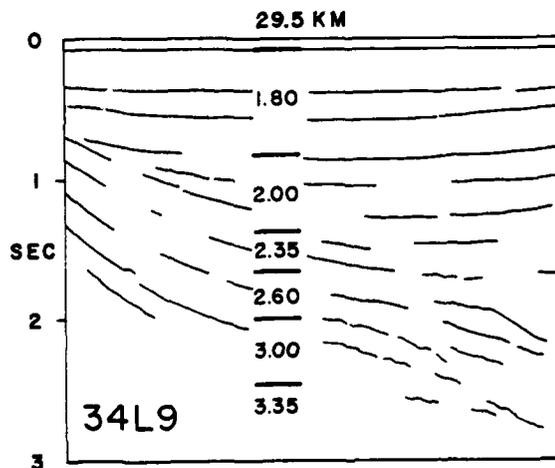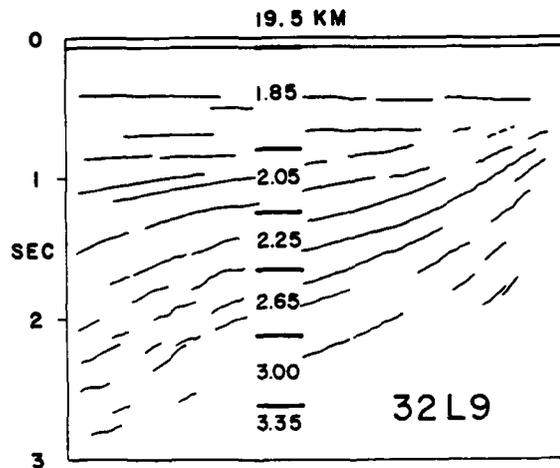
Fig. 4. Refraction solutions obtained from sonobuoy 32L9, shot up-dip, and 34L9, shot down-dip. The nearly identical structure sections demonstrate that the sound velocity depends on overburden and is unaffected by dipping bedding planes.
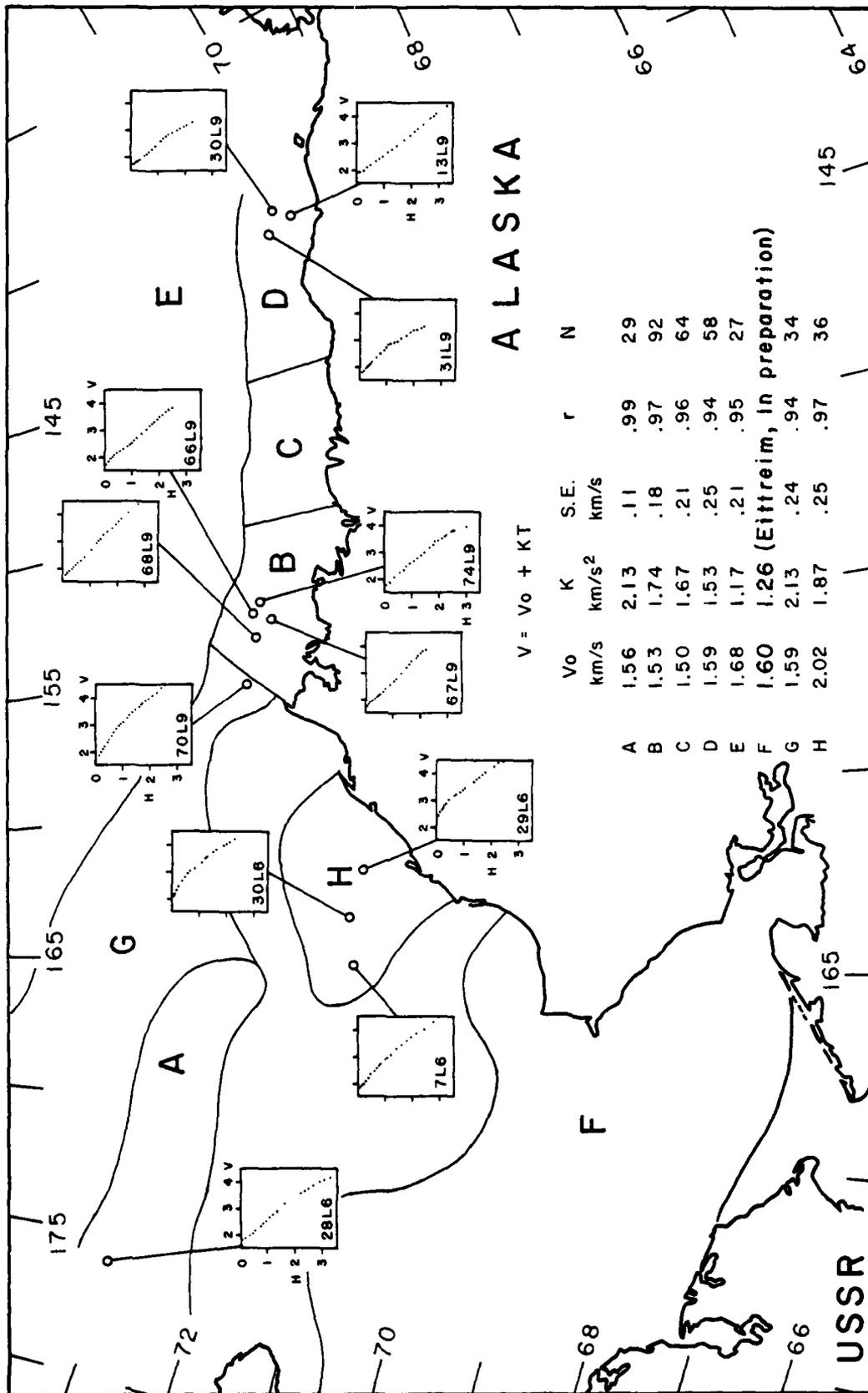
Fig. 5. Lettered regions are areas where the velocity functions shown in the table were determined. Insets show selected velocity-depth plots based on travel-time inversions.
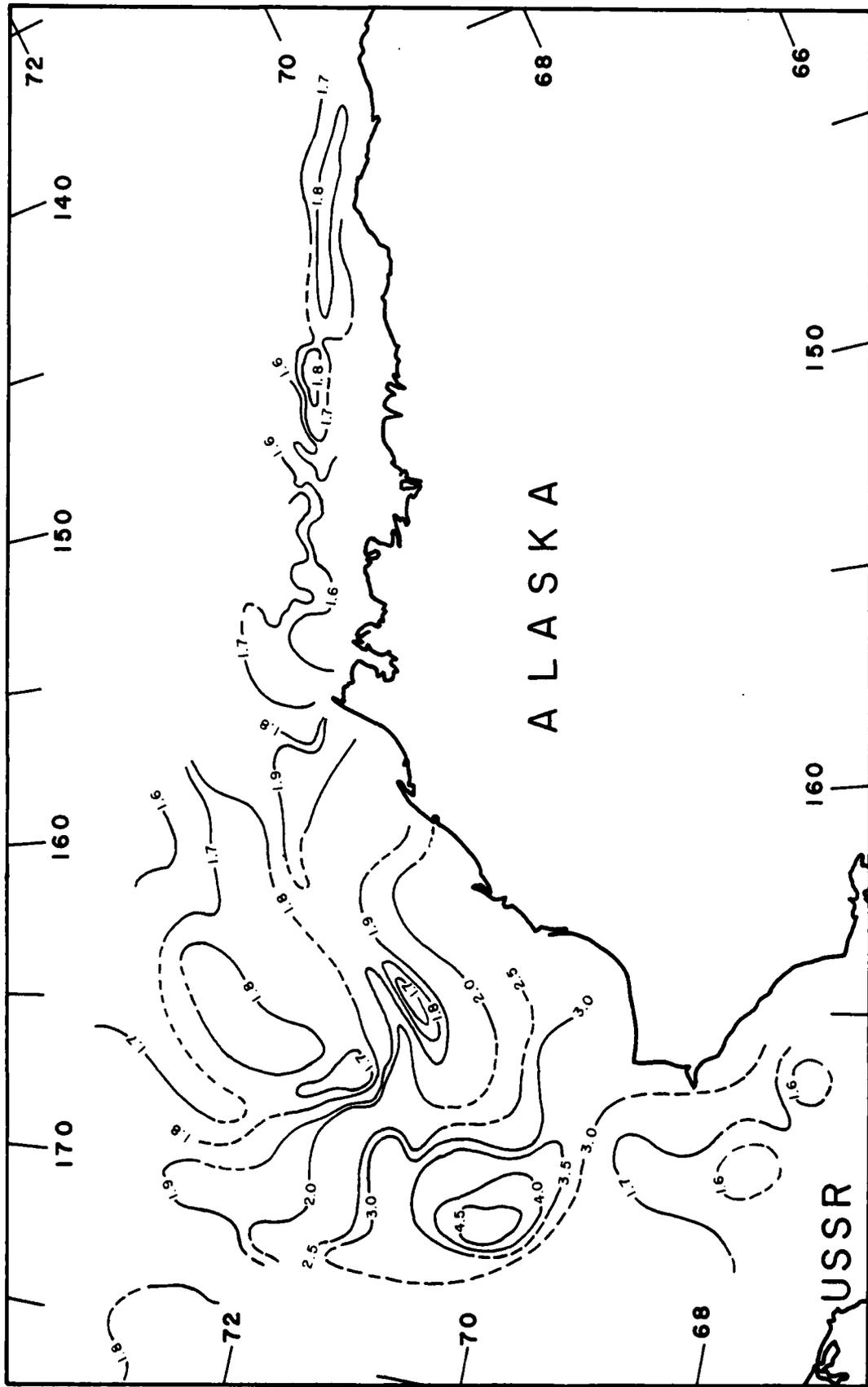
Fig. 6. Seafloor sound velocities contoured in units of km/s.
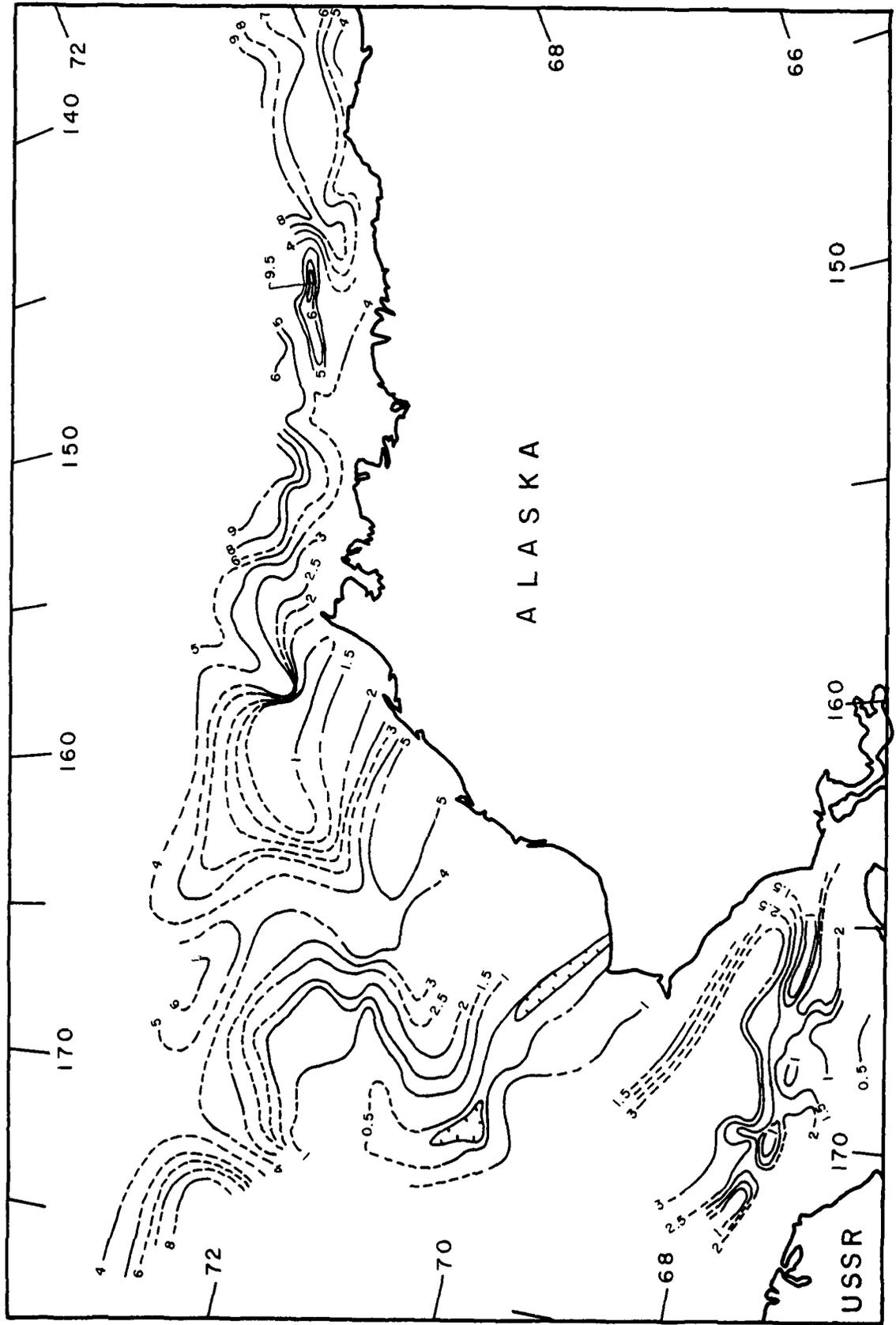
Fig. 7. Sediment thickness contoured in units of km. Hatched areas represent outcrops of high speed materials.

REPORT DOCUMENTATION PAGE		READ INSTRUCTIONS BEFORE COMPLETING FORM
1. REPORT NUMBER CU-2-79	2. GOVT ACCESSION NO. AD-A083621	3. RECIPIENT'S CATALOG NUMBER
4. TITLE (and Subtitle) Acoustic characteristics of the Shelves between Alaska and U.S.S.R.		5. TYPE OF REPORT & PERIOD COVERED Technical Report 5/79 to 10/79
		6. PERFORMING ORG. REPORT NUMBER
7. AUTHOR(s) Robert E. Houtz		8. CONTRACT OR GRANT NUMBER(s) N00014-75-C-1126
9. PERFORMING ORGANIZATION NAME AND ADDRESS L-DGO Palisades, N.Y. 10964		10. PROGRAM ELEMENT, PROJECT, TASK AREA & WORK UNIT NUMBERS
11. CONTROLLING OFFICE NAME AND ADDRESS Earth Physics Program, Office of Naval Research, Department of the Navy, Arlington, VA 22217		12. REPORT DATE 10/79
		13. NUMBER OF PAGES 21
14. MONITORING AGENCY NAME & ADDRESS(if different from Controlling Office)		15. SECURITY CLASS. (of this report) Unclassified
		15a. DECLASSIFICATION/DOWNGRADING SCHEDULE N/A

16. DISTRIBUTION STATEMENT (of this Report)

Approved for public release: distribution unlimited.

17. DISTRIBUTION STATEMENT (of the abstract entered in Block 20, if different from Report)

Approved for public release: distribution unlimited

18. SUPPLEMENTARY NOTES

19. KEY WORDS (Continue on reverse side if necessary and identify by block number)

Acoustics, sediments, shelf, sonobuoy, refraction.

20. ABSTRACT (Continue on reverse side if necessary and identify by block number)
Sound velocity characteristics at the seafloor and down to depths of 9-10 km have been generalized from 554 sonobuoy solutions in the Chukchi and Beaufort Seas. Sediment isopachs, contoured seafloor sound velocities, general geology, and velocity-depth functions appear in a set of regional charts.

DD ₁ FORM 1473   EDITION OF 1 NOV 68 IS OBSOLETE
   JAN 73
S/N 0102-LF-014-6601

MANDATORY DISTRIBUTION LIST
UNCLASSIFIED TECHNICAL REPORTS, REPRINTS, AND FINAL REPORTS
PUBLISHED BY CONTRACTORS OF THE
EARTH PHYSICS PROGRAM
OFFICE OF NAVAL RESEARCH

(October 1979)

Chief of Naval Research		Director
Department of the Navy		Defense Advanced Research
800 North Quincy Street		Projects Agency
Arlington, Virginia 22217 -		1400 Wilson Boulevard
Code 100C1	(1)	Arlington, Virginia 22209 (1)
Code 460	(1)	
Code 463	(5)	
Code 480	(1)	Air Force Office of
		Scientific Research
		Department of the Air Force
Commanding Officer		Directorate of Physics (MPG)
Office of Naval Research		Building 410
Branch Office	(1)	Bolling Air Force Base
* (ONR Branch Office for		Washington, D.C. 20332 (1)
contractor area)		

Army Research Office
Department of the Army
Geosciences Division
Box 12211

Director   Research Triangle Park,
Naval Research Laboratory   North Carolina 27709   (1)
Code 2627
Washington, D.C. 0375   (6)

                                        Defense Documentation Center
                                        Building 5
Office of Research, Develop-   Cameron Station
  ment, Test, and Evaluation   Alexandria, Virginia 22314   (12)
Department of the Navy
Code NOP-987J
Washington, D.C. 20350   (1)   Administrative Contracting
                                          Office (ACO)   (1)
                                        * (Given in Block 6 of
                                          Award/Contract Form
                                          26-103)

* Address to be determined by each contractor.

Enclosure 1

SUPPLEMENTARY DISTRIBUTION LIST
ONR CONTRACT NO. N00014-75-C-1126

(October 1979)

Dr. George H. Sutton
Hawaii Institute of Geophysics
University of Hawaii
2525 Correa Road
Honolulu, HI 96822

Dr. John Northrop
Naval Ocean Systems Center
Code 849
San Diego, CA 92152

Professor Jack Oliver
Cornell University
Department of Geological Sciences
McGraw Hall
Ithaca, NY 14850

Dr. Gary Latham
University of Texas
Marine Geophysical Laboratory
Galveston, TX 77550

Dr. Glenn McLeroy
Naval Coastal Systems Center
Code 791
Panama City, FL 32401

Mr. J. A. Ballard
Naval Ocean Research and
  Development Activity
Code 362
NSTL Station, MS 39529

Professor John I. Ewing
Woods Hole Oceanographic Institute
Woods Hole, MA 02543

Dr. Edwin L. Hamilton
Naval Ocean Systems Center
Code 8499
San Diego, CA 92152

Mr. Richard Hecht
Underwater Systems, Inc.
8121 Georgia Avenue
Silver Spring, MD 20910

Dr. Stephen N. Wolf
Naval Research Laboratory
Code 8121
4555 Overlook Avenue, SW
Washington, DC 20375

Dr. Lawrence Braile
Purdue University
Department of Geosciences
Lafayette, IN 47907

Dr. Ken Hawker
University of Texas at Austin
Applied Research Laboratory
P.O. Box 8029
Austin, TX 78712

Dr. Fred DiNapoli
Naval Underwater Systems Command
New London, CT 06320